

Theory of resonant stationary discharge with multiply charged ions in plasma flow propagating in mirror magnetic trap

I.S. Abramov, E.D. Gospodchikov, A.G. Shalashov

Institute of Applied Physics RAS, Nizhny Novgorod, Russia, abramov@appl.sci-nnov.ru
Lobachevsky State University of Nizhny Novgorod, Russia

Nowadays semiconductor industry requires reliable sources of extreme ultraviolet radiation (EUV) for next generation projection lithography [1]. In practical applications the only radiation fitting EUV spectral region is line radiation of multiply charged ions of Sn or Xe. These ions have considerable number of lines within the wavelength band of $13.5 \pm 1\%$ nm [2, 3] that corresponds to peak values of reflection coefficient for existing Mo/Si multilayer mirrors. The most advanced projects use laser produced plasma to obtain required ion charges [4, 5]. These facilities are characterized by about 4–5% conversion efficiency to $13.5 \pm 1\%$ nm band and total output of EUV radiation up to 250 W of averaged power.

Microwave discharge seems to be a perspective alternative to laser produced plasma. Pioneer experiments performed at IAP RAS (Nizhny Novgorod, Russia) demonstrated possibility of this plasma usage for generation of EUV radiation [6]. In the experiments, Sn plasma from vacuum arc source propagates in axial vicinity of the mirror magnetic trap. The flow is heated by 75 GHz / 50 kW gyrotron. The key feature of the experiments is resonant nature of plasma heating providing effective power load directly into the electron component that results in high rates of electron impact ionization and excitation without sufficient ion heating. In the paper we propose the theory of considered discharges that is of interest in terms of further source development.

Let us consider a plasma flow along confining magnetic field $B(x)$. The effective cross-section $\sigma(x)$ of the flow is unambiguously defined from the magnetic field line freezing-in, $B \sigma = \text{const}$. Plasma is characterized with the densities $n_j(x)$ of ions with charge-state $Z_j = j$, the flow velocity $u(x)$, the electron density $n_e(x)$ followed from the quasi-neutrality condition, and the effective electron temperature T_e . Variation of the electron temperature along the flow is neglected due to high electron thermal conductivity typical for high-power microwave discharge [7]. Electron temperature considerably exceeds the temperature of ions, thus we also neglect the ion pressure as compared to the electron pressure. Discharge duration is defined by the pulse length of the supporting microwave source which scales from 100 μs to CW. It is much longer than internal times of the discharge evolution, e.g. ion fly-time through the trap, so we consider a stationary discharge. Under these assumptions, we use the following fluid equations

$$\partial_x(\sigma n_j u) = \sigma(k_{j-1} n_e n_{j-1} - k_j n_e n_j), \quad (1)$$

$$\partial_x(\sigma \sum M n_j u^2) = \sigma \partial_x(n_e T_e), \quad (2)$$

representing the particle balance for ions and total ion and electron momentum balance [7, 8]. Here the sum is taken over all ion species, M is the ion mass, and k_j is the ioni-

zation coefficient of j -th ion fraction. Electron temperature T_e enters this model as a parameter. The boundary conditions are defined by the initial ion beam composition at the plasma gun, the ion beam current and the presence of the transition from the subsonic flow inside the trap to the supersonic one in the expanding region providing decreasing electron density needed for thermal insulation of the discharge. Formal mathematical difficulties considering dependence of this transition location on preceding ionization dynamics may be resolved as it is proposed in [8].

Power load that is needed to support the discharge may be estimated from the energy conservation

$$P(T_e) = A \sigma n u \frac{M u^2}{2} \Big|_{x \rightarrow \infty} + \int \sigma p_{\text{ion}} dx + \int \sigma p_{\text{exc}} dx. \quad (3)$$

The first term represents the convective losses, here $A \sim 2.5 - 5$ depending on the details of plasma absorber. Other terms describe the volumetric losses for ionization and line excitation of ions, characterized with densities

$$p_{\text{ion}} = \sum_j E_j k_j n_e n_j, \quad p_{\text{exc}} = \sum_j \sum_l \Delta E_{jl} k_{jl}^* n_e n_j. \quad (4)$$

Here p_{ion} is the power spent to ionize a unit volume of multiply charged plasma, E_j is the ionization energy and $k_j n_e$ is the effective rate of electron impact ionization for j -th ion, p_{exc} is the power spent to line excitation, inner sum is over allowed transitions in the spectrum of j -th ion, ΔE_{jl} and $k_{jl}^* n_e$ are the transition energies and rates. In the studied conditions, the rates of non-radiative processes and the photon trapping are low: once excited, an ion spontaneously relaxes to the ground state emitting a photon that leaves the discharge volume. So, with good accuracy, p_{exc} may be interpreted as radiation losses.

In the absence of data related to an electron distribution function formed in the discharge, we use monoenergetic cross-sections averaged over Maxwellian distribution. Fitting parameters for the electron-impact ionization processes in Sn plasma, presumably used for EUV radiation sources development, are taken from [9]. For the estimation of the excitation coefficients, Bethe approximation for dipole allowed transitions is used [10],

$$k_{jl}^* = 1.6 \times 10^{-5} \frac{\text{cm}^3}{\text{s}} \left[\frac{T_e}{1 \text{eV}} \right]^{-\frac{3}{2}} \frac{f_{jl} \langle g(\varepsilon_{jl}) \rangle}{\varepsilon_{jl} \exp(\varepsilon_{jl})}, \quad (5)$$

where $\varepsilon_{jl} = \Delta E_{jl} / T_e$, f_{jl} is the oscillator strength of corresponding transition. Function $\langle g(\varepsilon_{jl}) \rangle$ is averaged Gaunt-factor. In our model, we use Gaunt-factor in the form proposed in [11] and corrected in [12], see Fig. 1. The oscillator strengths are taken from NIST Atomic Spectra Database [13] for Sn^{+1} and, in the absence of such data that is typical for highly charged ions, calculated by Co-

wan's suite of codes [14]. Such calculations were performed for $\text{Sn}^{2+} - \text{Sn}^{19+}$. Results for EUV band are presented in Fig. 2 for several ion species. Only allowed transitions are taken into consideration in our model due to their higher probabilities and presence of numerous resonance lines ($\Delta n = 0$) in spectra of Sn ions that correspond to situation when allowed transitions dominate.

Discharge simulations within the model show relatively good agreement to available experimental data [6] realizing flow regimes with similar emitted EUV power and obtained ion charges.

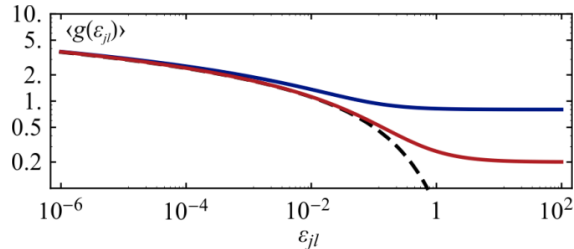


Fig. 1. Gaunt-factor $\langle g(\varepsilon_{jl}) \rangle$ averaged over Maxwellian distribution of electrons: red line – as formulated by Van Regemorter [13], blue line – after correction by Sampson and Zhang [14] (used in the modeling), black dashed line – high-temperature asymptotics given by $\sqrt{3}E_i(\varepsilon_{jl})/2\pi$

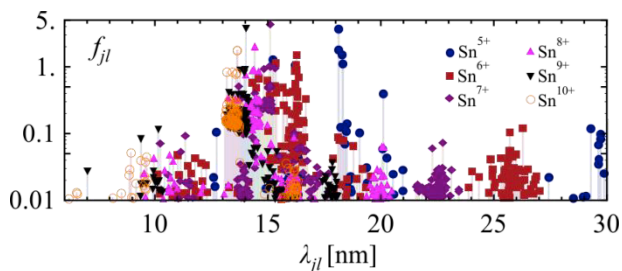


Fig. 2. Calculated oscillator strengths of allowed transitions in EUV spectral region for $\text{Sn}^{+5} - \text{Sn}^{+10}$. Ion species are indicated by different colors and unique geometric figure.

Modeling is performed in a wide range of plasma parameters and possible magnetic configurations taking into account physical constraints related to now available sources of microwave radiation and plasma. As a result, we find out opportunities for optimization of future EUV sources based on the discussed concept. An example of such optimization is illustrated in Fig. 3. The figure shows flow regime with an improved magnetic configuration. Such discharge emits about 40 kW of EUV radiation in $13.5 \pm 1\%$ nm with 20% conversion efficiency. The size of EUV emitting region is about $1 \text{ cm} \times 0.3 \text{ cm}^2$ what is far from the point-like source optimal for the beam forming optics. Therefore, some additional losses in efficiency may be expected due to not ideal EUV focusing; however, this is compensated by the very high emitting efficiency and total power of EUV radiation.

As a summary, we point out that scaling of the results of existing experiments on the microwave assisted EUV radiation in Sn plasma shows good potentials for the development of an industry-ready source featured with a

multi-kW level in $13.5 \pm 1\%$ nm band. Most required hardware, such as compact high-current plasma sources and high-power high-frequency gyrotrons, are available.

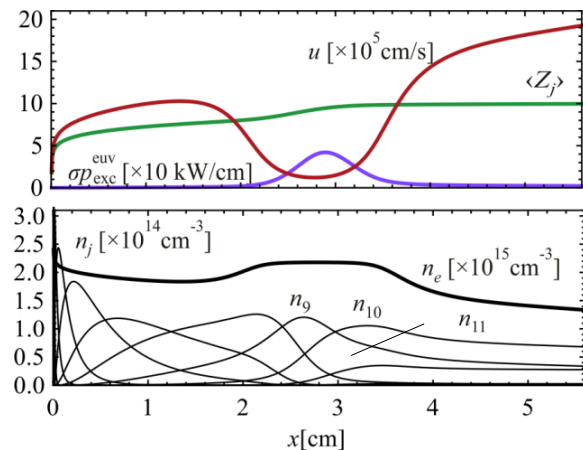


Fig. 3. Simulation of EUV-radiating discharge: variation along the trap axis of flow velocity u (red line, top panel), average ion charge $\langle Z_j \rangle$ (green line), linear power density σp_{exc} of radiation in $13.5 \pm 1\%$ nm EUV band (violet line), ion fractions' densities n_j (thin black lines, bottom panel), and electron density n_e (thick black line). Model parameters are: trap length $L = 5.6$ cm, mirror ratio $R = 9$, initial plasma diameter $d = 0.2$ cm, arc current $I_a = 2.9$ kA, initial beam composition $n_1(0)/\Sigma n_j(0) \approx 0.325$, $n_2(0)/\Sigma n_j(0) \approx 0.567$, $n_3(0)/\Sigma n_j(0) \approx 0.108$, and other components are negligible.

The work was supported by Russian Science Foundation (grant No. 14-12-00609).

References

1. C. Wagner, N. Harned, Nat. Phot. 2010. V. 4. P. 24.
2. S. Churilov, Y. N. Joshi, J. Reader, Optics Letters 2003. V. 28. P. 1478.
3. J. White, P. Hayden, P. Dunne et al. Journal of Applied Physics 2005, V 98, P. 113301.
4. A. A. Schafgans, D. Brown, I. Fomenkov et al. Proc. SPIE 2015. V. 9422. P. 94220B-1.
5. H. Mizoguchi, H. Nakarai, T. Abe et al. Proc. SPIE 2016. V. 9776. P. 97760J-1.
6. N. I. Chkhalo, S. V. Golubev et al. J. Micro Nanolithogr. MEMS MOEMS 2012. V. 11, P. 021123-1.
7. I. S. Abramov, E. D. Gospodchikov, A. G. Shalashov. Radiophysics and Quantum Electronics. V. 58. P. 914.
8. A. G. Shalashov, I. S. Abramov, S. V. Golubev, E. D. Gospodchikov. JETP 2016. V. 123. P. 219.
9. A. V. Philippov, V. M. Povyshev, A. A. Sadovoy et al. JINR Commun. 2002. V. E9-2002-5. P. 1.
10. J. D. Huba. NRL: Plasma formulary No. NRL/PU/6790-04-477 (2004). Eq. (4) on page 52.
11. H. Van Regemorter. The Astrophysics Journal 1962. V. 136. P. 906.
12. D. H. Sampson, H. L. Zhang. Phys. Rev. A 1992. V. 45. P. 1556.
13. A. Kramida, Yu. Ralchenko, J. Reader, and NIST ASD Team. NIST Atomic Spectra Database (v. 5.4). Available at <http://physics.nist.gov/asd> (NIST, Gaithersburg, MD, 2016).
14. R. D. Cowan. The theory of atomic structure and spectra (Univ. of California Press 1981)